A Linear State Estimation Formulation for Smart Distribution Systems

Daniel A. Haughton, *Student Member, IEEE*, and Gerald Thomas Heydt, *Life Fellow, IEEE*

***Abstract*—This paper presents a linearized, three-phase, distribution class state estimation algorithm for applications in smart distribution systems. Unbalanced three-phase cases and single-phase cases are accommodated. The estimator follows a complex variable formulation and is intended to incorporate synchronized phasor measurements into distribution state estimation. Potential applications in smart distribution system control and management are discussed.**

***Index Terms*—Distribution management systems, distribution system monitoring and control, distribution system state estimation, power distribution engineering, synchronized phasor measurements, three-phase unbalance.**

I. State Estimation in Distribution Systems

DISTRIBUTION system monitoring, automation, control and operation are key challenges facing the Smart Grid. Increased efficiency, reliability and flexibility may be achieved through enhancing these features of power distribution. Direct load control, demand response (DR), increased renewable electric generation, and sensory and communication networks are envisioned as part of the Smart Grid [1]. The cited Smart Grid objectives motivate the work reported in this paper, namely state estimation for distribution systems.

Characteristics of *conventional* distribution circuits include:

- radial operation;
- unbalanced loading inherent in systems with laterals consisting of 1 or 2 phase conductors;
- distributed loads separated by short distances;
- untransposed phase conductors;
- conductors with high r/x ratios;
- low penetration of distributed generation (DG), and no conventional generation;
- paucity of feeder measurements (low redundancy).

Further discussions are found in [2]–[6]. Three-phase unbalanced radial distribution power flow techniques based on ladder iterative, or similar, methods are generally employed for distribution system analysis [2]. However, as utilities tend toward smart distribution systems, the need for enhanced system monitoring and control based on real-time data becomes significant. Smart distribution systems are characterized as having higher penetration of DG, DR enabled loads, and controllable elements. Perhaps integral to the smart distribution system is the distribution management system (DMS) where an information technology (IT) layer allows for enhanced automation and control functions [3]. Distribution automation (DA) and DMS systems may generally include components of voltage/VAr control and outage management. Its transmission engineering analog, energy management system (EMS), is used extensively for near real-time analysis and control [4].

The need for state estimation at the distribution level is particularly acute in the smart distribution applications. For example, monitoring and situational awareness may become necessary for: circuits with active DG injection where potential bi-directional power flows may occur in each phase; exacerbation of voltage unbalance issues due to DG and stochastic loading; and assessment of system conditions after DR enabled loads respond to curtailment commands.

Previous approaches to the distribution state estimation formulation are discussed in [5]–[11]. In [5] a state estimation algorithm involves constraints on circuit quantities such as power factors, and real and reactive parts of substation transformer currents. Authors in [6] formulate an algorithm analogous to transmission state estimation for three-phase circuits. Use of branch current state vector was shown in [7], [8]; decoupling of phases and increasing computational efficiency are shown. A ladder iterative method employing branch current measurements is presented in [9]. Formulations discussed generally focus on low availability of real-time measurements, although [10] identifies the potential for improvements based on synchrophasor measurements widely deployed throughout the feeders.

Other key developments in state estimation include incorporation of synchronized phasor measurement devices [12]–[14] and smart meter devices [15], [16]. In transmission state estimation, the former enables effective wide-area monitoring for assessment of real-time system state. This is due to its ability to capture measurements in full phasor detail [12]. The latter has recently been adopted by utilities and is expected to drastically enhance monitoring and near real-time data availability for distribution networks. Also automatic meter-reading, remote connect/disconnect and DR initiatives, and variable pricing are enhanced [15], [16].

II. State Estimation Formulation for Electric Power Distribution Systems

State estimation is a mathematical tool in which a set of measurements is combined with an assumed mathematical model of a system so that the resulting set of equations relating measurements to the system are satisfied in the least squares sense. That is, the system states are estimated using an overdetermined set

Manuscript received January 12, 2012; revised April 30, 2012 and July 05, 2012; accepted August 03, 2012. Date of publication September 13, 2012; date of current version April 18, 2013. This work was supported by the Power Systems Engineering Research Center (PSerc), a Generation III Industry/University Cooperative Research Center, under grant NSF EEC-0001880 and EEC-0968993 and the Future Renewable Electric Energy Distribution and Management Center (FREEDM), an Engineering Research Center under grant NSF EEC-08212121. Paper no. TPWRS-00038-2012.

The authors are with the Department of Electrical, Computer, and Energy Engineering, Arizona State University, Tempe, AZ 85287 USA (e-mail: daniel.haughton@asu.edu; heydt@asu.edu).

Color versions of one or more of the figures in this paper are available online at http://ieeexplore.ieee.org.

Digital Object Identifier 10.1109/TPWRS.2012.2212921

of equations whose right- and left-hand sides agree with a minimum squared difference. Mathematically, the measurements are arranged in a vector z' and related to the system states x by the vector valued function (of vector valued argument) h

$$h(x) = z' + \eta \tag{1}$$

where η is a vector of noise (error) terms. Let the measurement vector incorporate noise terms and rewrite as

$$z = z' + \eta. \tag{2}$$

If $h(x)$ is linearized about an expected operating point, one obtains

$$hx = z \tag{3}$$

where the notation hx indicates the linear relationship between process matrix and state vector. Note that in (3), x, and z, are real valued vectors, and h, is a real valued matrix. Equation (3) is the basis of unbiased linear state estimation as applied in power engineering. The estimation is the result of the minimization of the Euclidian 2-norm of the vector

$$r = z - hx. \tag{4}$$

Namely the objective function is written as

$$J(x) = \sum_{k=1}^{n} (z_k - h_k(x))^2 = r'r \tag{5}$$

where k is an arbitrary measurement and n is the number of measurements. The minimum of $J(x)$ is found when

$$\frac{\partial J(x)}{\partial x} = \frac{\partial \left[\sum_{k=1}^{n} (z_k - h_k(x))^2\right]}{\partial x} = \frac{\partial r'r}{\partial x} = 0. \tag{6}$$

Note that the scalar, $J(x)$, is the sum of squares of residuals for each measurement. The estimate is found when

$$\hat{x} = [h^t h]^{-1} h^t z = h^+ z \tag{7}$$

where h^+ is referred to as the pseudoinverse of the matrix h. This is the unbiased, least squares estimator. Weighted estimation is utilized to bias results towards dependable measurements. When the weight is selected as the inverse of the variance, the maximum likelihood estimate is obtained [17]; therefore, accurate data with low variance receive high weight. Assuming independent, uncorrelated transducer errors, a diagonal weight matrix, W, is incorporated to produce a weighted solution for (7)

$$\hat{x} = [h^t W h]^{-1} h^t W z.$$

Note that when the measurement function is linear, or is effectively linearized, this calculation may be direct. The details of this mathematical tool and its applications have been widely reported in the literature of which [17]–[20] are a small sampling. The condition number of h is often cited as a measure of the sensitivity of estimates to noise. The process matrix condition number is calculated using

$$\kappa(h^t h) = \|h^t\| \|h\| = \frac{s_{max}}{s_{min}} \tag{8}$$

where $\|\cdot\|$ is the 2-norm and s_{max} and s_{min} denote max/min singular values, respectively [21].

Again, the main application of power system state estimation has been in transmission engineering and large scale system operation where calculation provides a best estimate of unmeasured parameters, noisy measured quantities, and other unmeasured nodes. In this case, the state estimator makes available to operators all salient system bus voltages, currents, and real and reactive power injections and flows. Perhaps the most evident application has been in the estimation of voltage and current phase angles which, prior to the advent of synchrophasor measurement technologies, have not been conveniently and synchronously measured.

III. Linear Three-Phase State Estimator

Attention turns to the development of a three-phase distribution state estimator. The basic design of the estimator is non-iterative, purely real, linearized and in full phase detail. In the distribution system application, it is assumed that coincident demands (e.g., smart meter [22]) and selected synchronous measurements will be used. In the formulation below, data shall be represented in complex, rectangular, phasor form. Three-phase unbalanced voltages and current measurements are envisioned along with some branch active and reactive power flow measurements. Measurement vector $z = z_r + jz_i$, the state vector $x = x_r + jx_i$, and the process matrix $h = h_r + jh_i$ are complex quantities where the subscripts r and i refer to real and imaginary components. Note that differentiation with respect to a complex variable is generally nonanalytic. Therefore (4) is rewritten

$$r_r + jr_i = (z_r + jz_i) - (h_r + jh_i)(x_r + jx_i). \tag{9}$$

Note that residual vector may be separated into real and imaginary parts

$$\begin{bmatrix} r_r \\ r_i \end{bmatrix} = \begin{bmatrix} z_r - h_r x_r + h_i x_i \\ z_i - h_r x_i - h_i x_r \end{bmatrix}. \tag{10}$$

Then, the minimization of the 2-norm may directly follow (6), where the state variables in this case are real-valued and partitioned into real and imaginary subvectors. Direct calculation for the 2-norm of a complex vector is

$$r^H r = (z_r - h_r x_r + h_i x_i)^2 + (z_i - h_i x_r - h_i x_i)^2. \tag{11}$$

The notation $(\cdot)^H$ refers to the Hermitian operation which is transposition followed by complex conjugation. Minimization of $r^H r$ entails the simultaneous solution of

$$\frac{\partial}{\partial x_r} r^H r = 0 \quad \frac{\partial}{\partial x_i} r^H r = 0.$$

Note that x_r and x_i are independent variables. Given an assumed voltage state vector for a distribution network, it may be practical to assume that bus voltage phase angle deviations for small changes in total feeder load are small. Linearization approximations in this estimator formulation exploit the small angle assumption.

The residual vector may be separated into real and imaginary components accordingly, thus producing a real-valued vector. In matrix form

$$\begin{bmatrix} h_r & -h_i \\ h_i & h_r \end{bmatrix} \begin{bmatrix} x_r \\ x_i \end{bmatrix} = \begin{bmatrix} z_r \\ z_i \end{bmatrix}.$$

The estimator then solves for the state estimate

$$\begin{bmatrix} \hat{x}_r \\ \hat{i} \end{bmatrix} = \begin{bmatrix} h_r & -h_i \\ h_i & h_r \end{bmatrix}^{+} \begin{bmatrix} z_r \\ z_i \end{bmatrix}. \tag{12}$$

The noise term is included in the measurement vector (2), and includes measurement device error, data transmission and other measurement errors. The linear estimator equations are developed here as

$$h = \begin{bmatrix} [Y_{BUS}] \\ [U] \\ [h_{LM}] \end{bmatrix} \quad \begin{bmatrix} [V_{meas}] \\ [I_{meas}] \\ [I_{line}] \end{bmatrix} \quad \hat{x} = [\hat{V}]$$

where

U identity matrix;

h_{LM} line measurement coefficient matrix;

Y_{BUS} system admittance model;

$V_{meas}, I_{meas}, I_{line}$ measurement vectors, in rectangular form;

I_{meas} measured and assumed injections/loads.

Full complex forms of the measurements in rectangular coordinates are used.

The Y_{BUS} is formed using three-phase block impedance representation of system components. Three-phase, four-wire line segments may be simplified by Kron reduction [2]. As a non-iterative solution procedure, there is little concern for instabilities caused by Newton-type iterative and fast decoupled methods when high r/x conductors are present [9], [17].

The advantages of a linear and non-iterative state estimation include: low computational burden, accommodation of meshed networks and avoidance of convergence issues (which may occur in dealing with systems with high r/x ratios).

IV. Distribution System Measurements in the Smart Grid Environment

A. Historical Data and Measurement Paucity

The measurement paucity, characteristic of conventional distribution systems, motivated some researchers to use historical data to supplant measurements to obtain an observable process matrix [5]–[9], [23]. However, reliance on historical data with insufficient measurement redundancy may produce inconsistent results when loading patterns deviate from history, or when unexpected outages and topology changes occur. In this case, the estimator may provide spurious results. Exploiting the available real-time data may fulfill the objective of enhanced decision making and control as envisioned for Smart Grid DMS and DA functions.

B. Smart Measurement Instruments

The state estimation formulation explored here exploits the advantages of the new technologies identified in Section I as they relate to distribution system engineering. That is, the data gathered from smart meters provide the requisite near real-time load measurement and potentially statistical data within short time intervals. Smart meters may record and transmit active and reactive power, energy consumption over time intervals, e.g., 5, 15, 60 min, and voltage magnitude data [16], [22]. Also, synchrophasors are envisioned to provide direct voltage phase angle measurement [12] for distribution buses. The practicality of this implementation is application dependant. Line power flows and current magnitudes may be ascertained via direct phasor quantity measurement. Note that standards [24] require measurement synchronization to within 1 μs, which corresponds to 0.0216° phase error in a 60-Hz system. Additionally, a maximum phase error of 0.57° produces total vector error (TVE), as defined in [24], of 1.0% which is the maximum allowable TVE.

C. Incorporation of Measurements

In the distribution state estimation formulation, it is assumed that both substation bus voltages and power flows (or current magnitudes) are always available. Other assumptions include sufficient availability of near real-time data (e.g., active and reactive power measurements, some voltage magnitudes and load power factors) to complement the estimator. The measurements may come from smart meters at loads and from distribution class synchrophasors at other buses. Assumed and measured load and DG injection currents are calculated. For example, a constant power load (other models may be used) current injection may be found using

$$I_{re}^{\varphi} = jI_{im}^{\varphi} = \frac{P^{\varphi} - jQ^{\varphi}}{V_m^{\varphi} \angle \left(-\delta_v^{\varphi}\right)} \tag{13}$$

where φ denotes the phase (a, b, c) and the voltage angle, δ, is assumed near nominal for that phase $(0^\circ, -120^\circ, 120^\circ)$, respectively, when not measured. If measured via synchrophasor, the measured δ^{φ}, or that of a nearby bus, may be used. Currents calculated in (13) are written in linear expressions in terms of the states, namely the bus voltages in rectangular notation. Substation active and reactive power flows may be expressed in terms of real and imaginary part of currents which are also linearly related to the states, particularly since substation bus voltage magnitude is known (as is impedance to the first load node). Other load models may be employed [2], [5], [23], [25]. Field tuning of load models may be required for verification, especially for power flow study accuracy. At the operating point, the solution to the system is linear, irrespective of load model used according to $YV = I$.

D. Selection of Weights for Calculated Measurements

The selection of weights for calculated, linearized currents may be approximated mathematically or determined heuristically. Measured P, Q, V_m and δ_v are random variables each with an expected value and variance [26]. Approximate expressions for mean and variance of calculated currents, (13), may be obtained when measurements are treated as independent random variables. The expected values of measured variables are $M = \{P, Q, V_m, \delta\}$, and their variance is chosen based on transducer accuracy. Attention now turns to the approximation of variance of the calculated current.

The expectation of real and imaginary parts of I ($\mu_{I_{re}}, \mu_{I_{im}}$, respectively) may be approximated from the nonlinear function

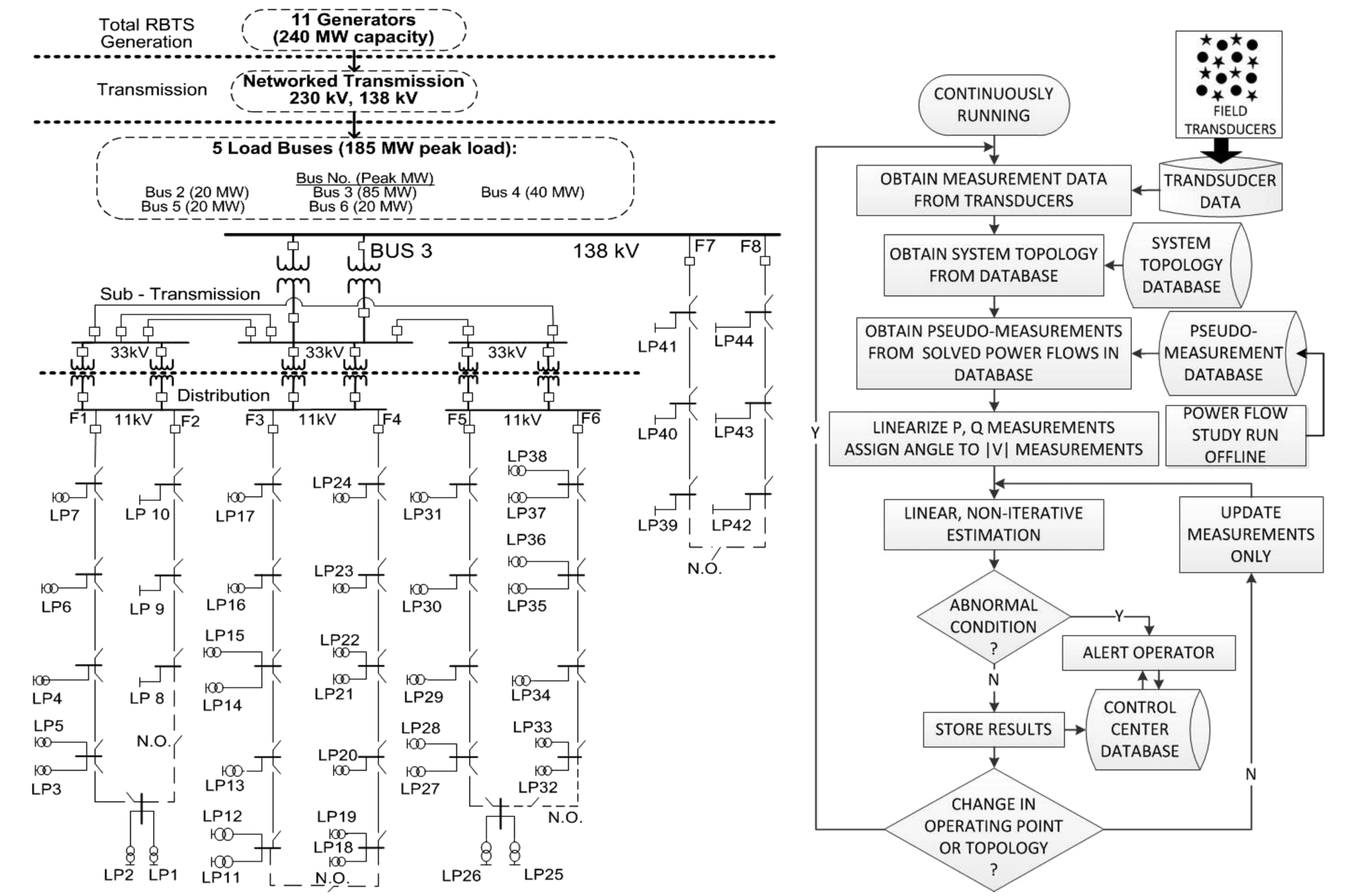

Fig. 1. (Left) RBTS one-line diagram showing bus 3 distribution subsystem and load points (LP), recreated from [34]; and (right) flowchart for the state estimation algorithm that runs continuously at the distribution substation.

(13). The variance of I_{re} (and similarly I_{im}) may be approximated from the Taylor series expansion, also commonly referred to as the delta method [26]

$$Var_{I_{re}} \cong \sum_{i=1}^{n} \left[\left(\frac{\partial \mu_{I_{re}}}{\partial M_i} \right)^2 Var_i \right]. \tag{14}$$

Variance of I_{im} is similarly approximated. Alternatively, a heuristic approach may be taken: the variance of I_{re} and I_{im} may be approximated by choosing a value corresponding to the largest variance (normalized) of all random variables, i.e., truncate the sum in (14) to only the largest term.

V. Distribution Management and the Smart Grid

Distribution state estimation has applications in the DMS and DA system considering a number of likely Smart Grid features including: electronic controllable elements on feeders; integration of DG (e.g., rooftop PV and small wind farms); DR controlled loads; and variable end-user pricing. Specific applications may include: identifying problematic operating conditions, monitoring branch flows for overloads, assessing bus voltage magnitudes for limit violations, DR switching status, and feeder voltage regulation. State estimation data and enhanced applications may all contribute to situational awareness as they function to make operators cognizant of near real-time grid status [27], [28].

The distribution class state estimator is proposed as a partial source of operating data to implement Smart Grid type controls. The estimator in this facet becomes a communication tool for all elements across the feeder. Implementation may consist of a DMS installed at a distribution substation that combines supervisory control and data acquisition (SCADA) data and feeder measurements. Potential applications in a DMS with enhanced state estimation capability include:

- reactive power dispatch to effectuate voltage regulation (e.g. capacitor, reactor or electronic load switching that permit reactive power control);
- electronic controls adapted to distribution circuits (distribution analog of FACTS) [29]–[31];
- adaptive protective devices;
- adaptive controls for DG [32], including inverter based devices, to accommodate limited, local voltage regulation (as presently disallowed in [33]);
- a supplementary tool to enhance optimization methods for distribution feeders using real-time data (reconfiguration, DG settings, voltage controls);
- near real-time pricing signals and to provide status of DR enabled load response.

VI. Illustrative Examples and Sample Results

A. Test Bed and Example Descriptions

Fig. 1 presents the one-line diagram for a sample distribution test system, denominated RBTS after its creator Roy Billinton [34]. Voltages range from 400 V–138 kV. Feeder F1 of this

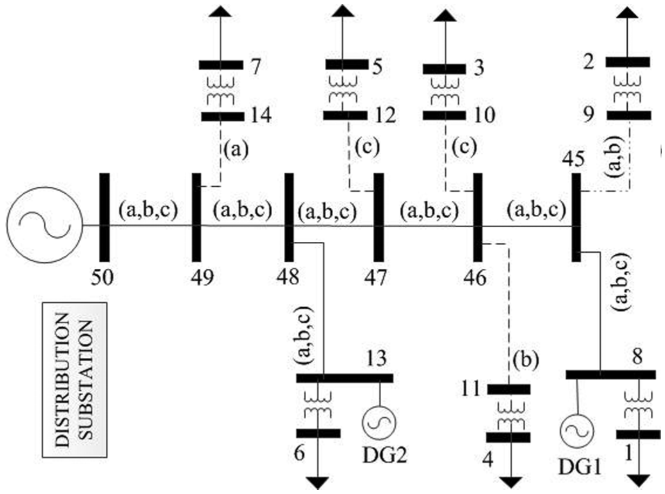

Fig. 2. One-line diagram of modified RBTS three-phase Feeder F1 with DG.

TABLE II
DEMANDS AT HEAVY LOAD, RBTS FEEDER F1

	Load					
LP	P (MW)			Q (MVAr)		
	A	B	C	A	B	C
1	0.470	0.450	0.390	0.220	0.200	0.150
2	0.470	0.490		0.230	0.250	
3			0.450			0.230
4		0.450			0.218	
5			0.450			0.218
6	0.450	0.510	0.450	0.240	0.250	0.200
7	0.450			0.220		
Total	1.84	1.90	1.74	0.910	0.918	0.798

system is modified to represent a three-phase unbalanced distribution circuit with DG as shown in Fig. 2. Note that laterals may contain single and two phase conductors and loads/load points (LP). Conductor details are provided in Table I. Power and voltage bases are 100 MVA, 11 kV, and 415 V. Note the r/x ratio of the 11 kV conductors is approximately 0.35. The examples presented subsequently demonstrate the performance of the linear, three-phase, unbalanced distribution system state estimator on the circuit of Fig. 2, and applications in a smart distribution system environment with significant DG penetration.

In the state estimation algorithm, bus voltage magnitude and aggregate load active and reactive power measurements are available at buses 2, 5, and 6. Synchrophasor voltage measurements are assumed at buses 11, 14 distribution transformer primary, and main feeder buses 45, 46, and 48. At load points where no measurement devices are present (aggregate load unknown), an algorithm is used to apportion the unmeasured load based on historical loading and reasonable assumptions at the load point. Power flows measured at the substation

$$P_{sub} = \sum_{i=1}^{n} P_i + P_{losses} \tag{15}$$

where n is the number of buses, and P_{losses} may be unknown or approximate. Measured bus loads total

$$P_{meas} = \sum_{l=1}^{k} P_l \tag{16}$$

where k is the number of measured load points. When substation active power flow changes are observed

$$\Delta P_{sub} = \sum_{i=1}^{n} \Delta P + \Delta P_{losses}. \tag{17}$$

TABLE I
CONDUCTOR DATA FOR RBTS FEEDER F1

Voltage (kV_{11})	Max. load current (A)	Ampacity (A)	R (Ω/mi)	X @ 1' spacing (Ω/mi)
11	292	800	0.140	0.412

TABLE III
DEMANDS AT LIGHT LOAD, RBTS FEEDER F1

	Load					
LP	P (MW)			Q (MVAr)		
	A	B	C	A	B	C
1	0.093	0.100	0.098	0.033	0.030	0.020
2	0.150	0.163		0.035	0.038	
3			0.100			0.035
4		0.093			0.032	
5			0.125			0.037
6	0.118	0.128	0.113	0.036	0.038	0.030
7	0.103			0.033		
Total	0.463	0.483	0.435	0.137	0.138	0.122

Aggregate unmeasured demands are approximated via

$$P_{unmeas} + P_{losses} = P_{sub} - P_{meas}. \tag{18}$$

Then, when substation power flow and measured loads change, the corresponding change in unmeasured aggregate load and subsequently unmeasured individual loads (historical or assumed) may be approximated

$$\Delta P_{unmeas} = \Delta P_{sub} - \Delta P_{meas} \tag{19}$$

$$\Delta P_{i\_unmeas} = P_{i\_unmeas} \left(\frac{\Delta P_{unmeas}}{P_{unmeas}} \right). \tag{20}$$

Limitations and weights based on historical data or installed capacity may be imposed. However, care must be taken in limiting load estimation due to the highly stochastic nature of the individual instantaneous load. In the longer time horizon, load growth may need to be considered. Reactive power assumptions also follow (15)–(20), and total feeder power factor change can be used to check accuracy of assumptions.

Load values at peak and light load conditions are provided in Tables II and III. Note that total substation load is generally balanced in each case, but feeder loading is unbalanced. A power flow solution under heavy loading condition produces significantly unbalanced voltage magnitudes as shown in Fig. 3, with voltage rise due to unbalanced loading and mutual coupling effects. It is assumed that light loading occurs at hour ending (HE) 3, heavy loading at HE 18, indicated in Fig. 4. Input loading data to the estimator (i.e., demands during some time interval) are combined with real-time bus voltage magnitude and synchrophasor measurements. The estimator performance is tested by first assuming average individual and substation loads in a given operating hour, e.g., the HE A are known. Based on changes to both total substation load and measured loads in HE B, non-metered loads are modified (15)–(20) and the system state at HE B is estimated. Note that some of the states are measured directly with synchrophasors, with angles relative to a reference bus.

B. Examples Explained

The examples EX1a, EX1b, EX2 and EX3 are described subsequently. In example EX1a, the static system state for HE 5 loading condition (unknown) is estimated, with only a few loads and bus voltages measured real-time. Measured voltages and

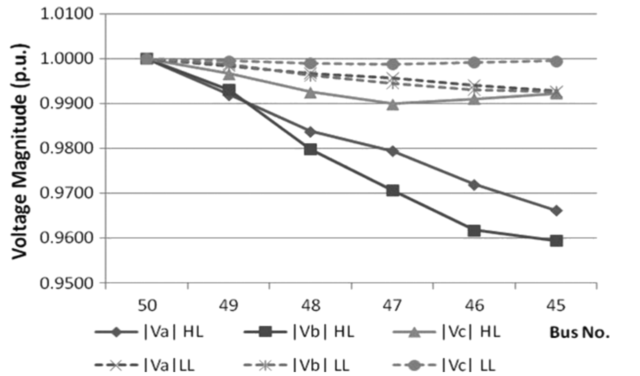

Fig. 3. Main feeder bus voltage magnitudes at heavy load (HL) and light (LL) load, RBTS feeder F1 (all examples).

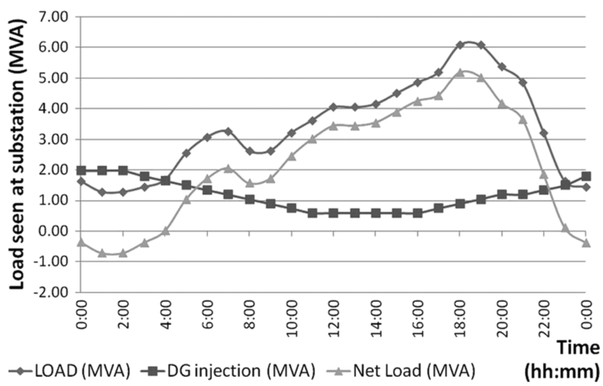

Fig. 4. RBTS feeder F1 peak day hourly load profile (all examples).

TABLE IV
BUS VOLTAGES USED IN EX1A, EX1B, AND EX2

Bus No.	Phase	Voltage (magnitude / angle, per unit, degrees)	
		EX1a, EX1b	EX2
2	(a)	0.9907 /-0.62	0.9820 /-1.34
	(b)	0.9914 /-120.95	0.9826 /-121.92
5	(c)	0.9972 / 119.38	0.9952 / 118.73
6	(a)	0.9950 /-0.42	0.9903 /-1.01
	(b)	0.9945 /-120.53	0.9899 /-121.13
	(c)	0.9979 / 119.51	0.9954 / 118.90
11†	(b)	0.9924 /-120.55	0.9842 /-121.33
14†	(a)	0.9980 /-0.13	0.9959 /-0.36
45†	(a)	0.9928 /-0.30	0.9857 /-0.77
	(b)	0.9927 /-120.57	0.9848 /-121.31
	(c)	0.9995 / 119.61	0.9989 / 119.01
46†	(a)	0.9941 /-0.25	0.9880 /-0.64
	(b)	0.9930 /-120.49	0.9855 /-121.15
	(c)	0.9992 / 119.60	0.9986 / 119.03
48†	(a)	0.9967 /-0.17	0.9933 /-0.44
	(b)	0.9963 /-120.25	0.9926 /-120.57
	(c)	0.9990 / 119.76	0.9979 / 119.44

† Angles measured directly with synchrophasors (others obtained from solved power flows). All voltages converted to rectangular form to be used in (12).

pseudo-measurement "angles" from power flow studies used for EX1a, EX1b, and EX2 are shown in Table IV. Load active and reactive demands used for the examples are shown in Table V. Note that not every bus has metered demand.

It is assumed that values for all loads at HE 3 are known and that the power flow solution values are available to supplement assumptions about non-metered loads (i.e., based on historical loading). EX1b assumes values from HE 7. No DG injections are assumed for this example. Example, EX2 provides estimator

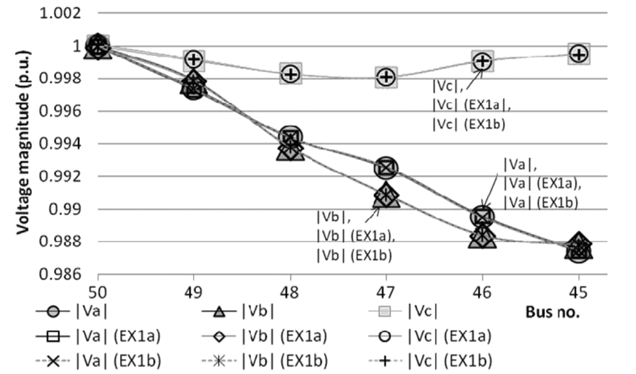

Fig. 5. Main feeder voltage magnitudes in HE5; exact data depicted from a three-phase power flow study, EX1a, EX1b.

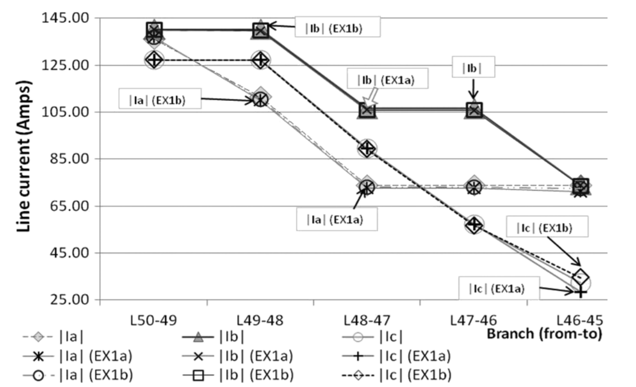

Fig. 6. Main feeder line current magnitudes; HE5 exact data depicted from a three-phase power flow study, EX1a, EX1b.

output results for heavy loading (HE 18) when exact loading for HE 3 (low load) only, is known. Example, EX3 includes DG on the circuit of Fig. 2. Each DG unit injects equal power at unity power factor, providing a total injection as identified by Fig. 4.

Additionally, Section IV-D demonstrates improved estimator performance when biased estimation is employed. Section VI-E provides a comparison of the estimator formulation presented here with conventional state estimation formulation. Section VI-F illustrates a bad data detection algorithm applied to the measurement set when a bad datum is introduced.

C. Sample Results: Unbiased Estimation

The estimator algorithm provides good estimation of static state at HE 5 load for EX1a and EX1b; bus voltage magnitudes and line current magnitudes are shown in Figs. 5 and 6. The error histogram for the worst case result, corresponding to EX1a, of voltage magnitude estimation is shown in Fig. 7.

Conversely, HE7 loading condition is much closer to HE5 (both real and reactive demands); therefore, the error in estimates for EX1b is greatly reduced. Fig. 8 shows voltage phase angle error histogram; note that initial load assumptions for HE3 also produce the worst case angle estimates. Fig. 9 shows the histogram for the line current magnitude errors calculated from state estimates. Maximum error in current magnitude occurs on phase A, at the main feeder section farthest from the substation, 4.5 amperes (15%). Fig. 10 shows line current phase angle error histogram for EX1a.

In example EX2, the state vector at peak, HE18, is estimated based on load assumptions (known states and loads) at low load, HE3. Estimated bus voltage magnitudes and angles are shown in

TABLE V
DEMAND AT EACH BUS USED IN EX1A, EX1B, AND EX2

Bus No. / EX.	Demand at each bus (P/Q in MW/ MVAr)						
	1†	2	3†	4†	5	6	7†
Power flow	0.600 / 0.125	0.500 / 0.125	0.155 / 0.030	0.200 / 0.040	0.200 / 0.050	0.665 / 0.175	0.150 / 0.045
EX1a, EX2	0.549 / 0.111	0.607 / 0.095	0.180 / 0.042	0.192 / 0.044	0.216 / 0.040	0.678 / 0.134	0.184 / 0.043
EX 1b	0.594 / 0.116	0.347 / 0.125	0.136 / 0.039	0.200 / 0.040	0.219 / 0.039	0.594 / 0.162	0.175 / 0.045

† Pseudomeasurement—demand calculated based on measurements at other buses and the substation according to (15)–(20). Metered (measured) values are shown in shaded columns.

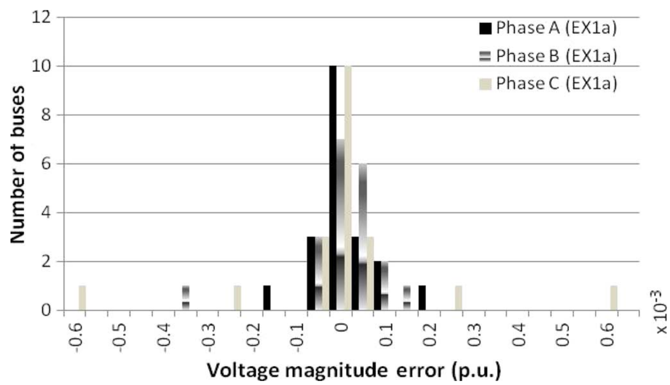

Fig. 7. Voltage magnitude error histogram (i.e., difference between estimate and three-phase power flow study), EX1a.

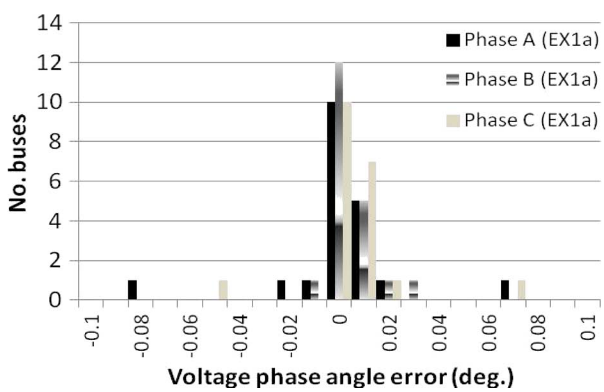

Fig. 8. Voltage angle error histogram (i.e., difference between estimate and three-phase power flow study), EX1a.

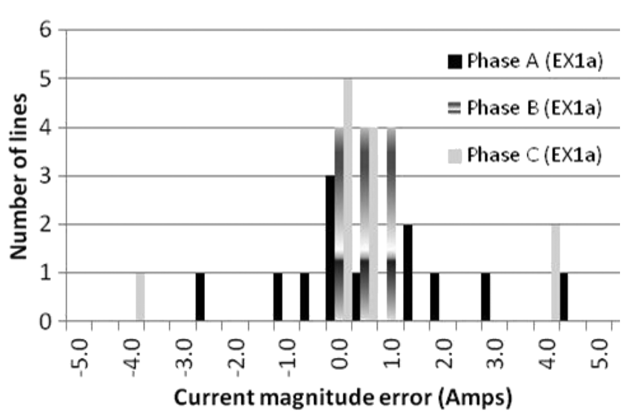

Fig. 9. Current magnitude error histogram (i.e., difference between estimate and three-phase power flow study), EX1a.

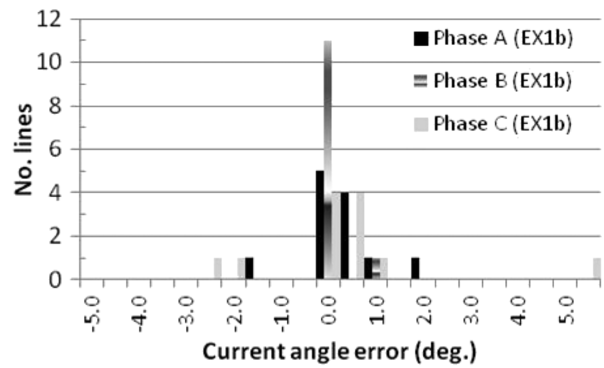

Fig. 10. Line current phase angle error histogram (i.e., difference between estimate and three-phase power flow study), EX1b.

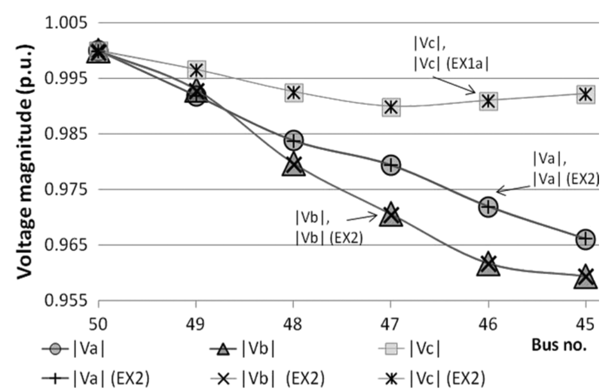

Fig. 11. Main feeder bus voltage magnitudes, feeder loading at HE18, exact and estimated, EX2.

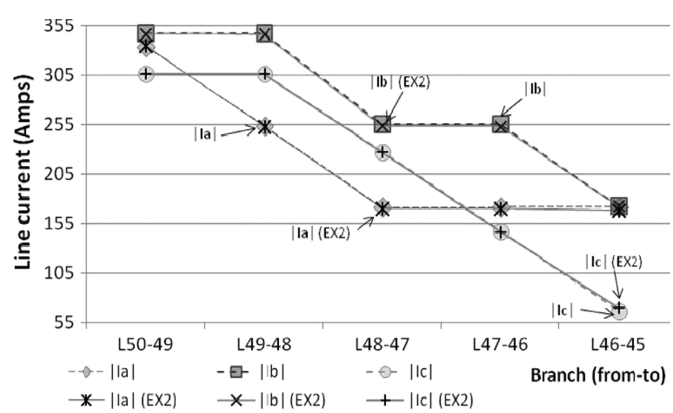

Fig. 12. Line currents for HE18 loading, exact (from three-phase power flow study) and estimated, EX2.

Figs. 11 and 12. The maximum absolute voltage magnitude and phase errors in this case are 0.0009 p.u. and 0.062°. Maximum line current magnitude error is 6.88 Amps (8.0%) in phase A at the load farthest from the source.

Example EX3 demonstrates an extreme case of bidirectional power flows when DG is present in a distribution feeder. DG injections in this simulation are 0.3 MW/phase at buses 13 and bus 8 of Fig. 2 at light load. Results in Fig. 13 show bidirectional flows in various phases at low load (HE3). The estimator

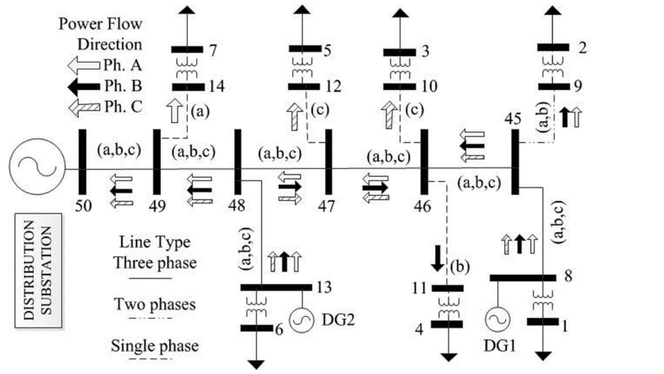

Loads / DG

Bus No.	Ph. A	Ph. B (MW)	Ph. C	Ph. A	Ph. B (MVAr)	Ph. C
1	0.09	0.10	0.10	0.03	0.03	0.02
2	0.15	0.16	0.00	0.04	0.04	0.00
3	0.00	0.00	0.10	0.00	0.00	0.04
4	0.00	0.09	0.00	0.00	0.04	0.00
5	0.00	0.00	0.12	0.00	0.00	0.03
6	0.12	0.13	0.11	0.04	0.04	0.03
7	0.10	0.00	0.00	0.03	0.00	0.00
DG1	0.33	0.33	0.33			
DG2	0.33	0.33	0.33			

Fig. 13. RBTS Feeder F1 with DG and bidirectional flows at HE3.

incorporating synchronized measurements is able to capture the bidirectional flows on the distribution circuit.

Note that active power flows in sections 46–47 and 47–48 are in opposing directions in each phase. Synchronized phasor measurements that capture angle information are extremely useful here. Impacts to protection coordination, voltage regulation and circuit operation exist [32] but are not addressed here. Obtaining angle information at these buses, helps ascertain power flow directions, even when angles difference across buses is fairly small.

The condition number of the $h^t h$ matrix for EX1a, EX1b, and EX2 is found to be 5133 indicating a well conditioned process matrix for this study [21]. Note that the system topology and measurement locations remain the same in each case, hence the same condition number is obtained. Weighting accurate measurements may produce larger condition numbers. However, the formulation presented here is shown to have no adverse effect on process matrix condition.

D. Sample Results: Biased Estimation

Example EX1 is repeated using the diagonal weight matrix, W in (7). In this illustration, standard deviations of measurements are taken as 3.0% for "smart meters"; 1.0% for synchrophasors; 50% for pseudo-measurements; and 0.5% for known zero current injections. Under the assumption of maximum likelihood, the measurement weights are the inverses of the corresponding variances [4], [11]. Sample results and impact on estimator accuracy are shown in Table VI.

E. Sample Results: Comparison to Conventional Estimation

Comparison to conventional positive sequence state estimation algorithms [11], [17], [18] is illustrated here. Three-phase solution detail is lost since loads and lines are assumed to be balanced three-phase. Impedances and loads are adjusted accordingly. Results shown in Table VII identify maximum error of estimated states versus a power flow solution. The relative time to solve conventional versus three-phase linear, non-iterative estimation is also shown. Note that the linear, non-iterative formulation provides greater solution detail (three-phase bus voltages) in comparable solution time [larger h matrix (7)] as opposed to assumed balanced conditions. In this case, the conventional estimator takes 3 iterations to solve.

References [6], [7], [11], and [23] also provide results for other estimation methods, including WLS, applied to positive sequence or three-phase test systems of similar size as the system studied here.

TABLE VI
RESULTS OBTAINED FROM BIASED MEASUREMENTS

EX	Max Voltage Error (%)		Max Current Error (%)		Improved accuracy
	Magnitude	Angle	Magnitude	Angle	
EX1a	0.013	1.10	4.50	3.70	85 %
EX1b	0.007	1.10	1.40	1.50	85 %
EX2	0.036	0.70	1.65	0.71	80 %

TABLE VII
COMPARISON TO CONVENTIONAL WLS ESTIMATION

		EX1a	EX1b	EX2
Max Voltage Error (%)	Magnitude (p.u.*10^{-3})	4.46	3.95	0.219
	Angle (deg.)	0.12	0.07	0.17
$t_{\text{conventional}}$ / $t_{\text{non-linear}}$		1.25	1.37	1.1
No. iterations		3	3	3

TABLE VIII
SAMPLE BAD DATA DETECTION RESULTS ON EX2

Example	$J(x)$	Detection threshold $\chi^2_{0.95,24}$	Bad data suspected
EX2 (unbiased)	9.95*10^{-4}	36.42	No
EX2 (biased)	19.41	36.42	No
EX2 (bad data)	81.42	36.42	Yes

F. Sample Results: Bad Data Detection Using Example EX2

Bad data detection and identification may be employed to filter the measurement set for erroneous data, provided that certain conditions are met (e.g., [17]). In this formulation, bad data detection and identification follow methods outlined in the classical literature. Bad data detection is investigated here using the well known chi-squared test. The chi-squared test is applied to the examples shown. The measurement set comprises all types of measurements used. A confidence level (e.g., 95%) is selected, and degrees of freedom equal to the difference between number of measurements and states. Sample results are presented for EX2 with phase A load at bus 2 set to 50% of its true value. Results are shown in Table VIII.

VII. CONCLUSIONS AND FINAL REMARKS

The well known weighted least squares method is used to develop a linear, non-iterative power system static state estimator for three-phase unbalanced distribution systems. The estimator is envisioned as a tool to aid system monitoring, automation and control efforts in a Smart Grid environment. Decision making based on real-time information communication and better control algorithms are made possible.

The formulation presented and examples incorporate smart meter data and synchronized phasor measurements at the primary distribution level. Estimator performance is illustrated on a range of feeder loading conditions. Biasing measurements is shown to increase expected accuracy. In the examples shown, relying on trusted measurements results in nearly an order of magnitude accuracy improvement in voltage magnitude and angle estimates, and also reduced calculated current magnitude errors from 15% down to 4%.

Knowledge of bus voltage phase angle from synchronized phasor measurements improves the state estimation process for power systems, and is shown here for distribution circuits. The practicality of large scale deployment of synchrophasor measurements in distribution systems is unknown. Direct measurement of bus voltage angle may be useful in distribution circuits for ascertaining power flows (both directions and magnitudes). DG injections and loading conditions of feeders may create an interesting case of bidirectional power flow.

The estimator formulation presented here is shown to be comparable to conventional estimation formulation of positive sequence quantities only, but the proposed formulation has the advantage of providing full three-phase detail. Bad data detection is illustrated on the test system.

REFERENCES

[1] Office of Electric Transmission and Distribution, United States Department of Energy, Grid 2030: A National Vision for Electricity's Second 100 Years. Washington, DC, Apr. 2003.

[2] W. H. Kersting, *Distribution System Modeling and Analysis*, 2nd ed. New York: CRC, 2007.

[3] J. Northcote-Green and R. G. Wilson, *Control and Automation of Electrical Power Distribution Systems*. Boca Raton, FL: CRC, 2006.

[4] A. J. Wood and B. F. Wollenberg, *Power Generation Operation and Control*, 2nd ed. New York: Wiley, 2007.

[5] I. Roytelman and S. M. Shahidehpour, "State estimation for electric power distribution systems in quasi real-time conditions," *IEEE Trans. Power Del.*, vol. 8, no. 4, pp. 2009–2015, Oct. 1993.

[6] M. E. Baran and A. W. Kelley, "State estimation for real-time monitoring of distribution systems," *IEEE Trans. Power Syst.*, vol. 9, no. 3, pp. 1601–1609, Aug. 1994.

[7] M. E. Baran and A. W. Kelley, "A branch-current based state estimation method for distribution systems," *IEEE Trans. Power Syst.*, vol. 10, no. 1, pp. 483–491, Feb. 1995.

[8] C. N. Lu, J. H. Teng, and W. E. Liu, "Distribution system state estimation," *IEEE Trans. Power Syst.*, vol. 10, no. 1, pp. 229–240, Feb. 1995.

[9] R. Hoffman, "Practical state estimation for electric distribution networks," in *Proc. IEEE Power Systems Conf. Expo.*, Oct. 2006, pp. 510–517.

[10] A. P. S. Meliopoulos and F. Zhang, "Multiphase power flow and state estimation for power distribution systems," *IEEE Trans. Power Syst.*, vol. 11, no. 2, pp. 939–946, May 1996.

[11] R. Singh, B. C. Pal, and R. A. Jabr, "Choice of estimator for distribution system state estimation," *IET Gen., Transm., Distrib.*, vol. 3, no. 7, pp. 666–678, Jul. 2009.

[12] A. G. Phadke and J. S. Thorp, *Synchronized Phasor Measurements and Their Applications*. New York: Springer, 2010.

[13] A. Abur, "Impact of phasor measurements on state estimation," in *Proc. Int. Conf. Electrical and Electronics Engineering*, Nov. 2009, pp. I3–I7.

[14] A. G. Phadke, "Synchronized phasor measurements—A historical overview," in *Proc. IEEE Transmission and Distribution Conf. Expo. Asia Pacific*, Yokohama, Japan, Oct. 2002, vol. 3, pp. 476–479.

[15] D. Wight *et al.*, Assessment of Demand Response and Advanced Metering Staff Report, U.S. Federal Energy Regulatory Commission, Feb. 2011.

[16] S. Mak, "Smart meters serving as synchro-sensors for smart distribution grid applications," in *Proc. IEEE PES General Meeting*, Detroit, MI, Jul. 2011.

[17] A. Abur and A. Gómez Expósito, *Power System State Estimation: Theory and Implementation*. New York: Marcel Dekker, 2004.

[18] A. Monticelli, "Electric power system state estimation," *Proc. IEEE*, vol. 88, no. 2, pp. 262–282, Feb. 2000.

[19] O. Alsac, N. Vempati, B. Stott, and A. Monticelli, "Generalized state estimation," *IEEE Trans. Power Syst.*, vol. 13, no. 3, pp. 1069–1075, Aug. 1998.

[20] R. E. Larson, W. F. Tinney, L. P. Hajdu, and D. S. Piercy, "State estimation in power systems part II: Implementation and applications," *IEEE Trans. Power App. Syst.*, vol. PAS-89, no. 3, pp. 353–363, 1970.

[21] R. Ebrahimian and R. Baldick, "State estimator condition number analysis," *IEEE Trans. Power Syst.*, vol. 16, no. 2, pp. 273–279, May 2001.

[22] Itron, Smart Meter Specifications Data Sheets, 2011. [Online]. Available: http://www.itron.com.

[23] E. Manitsas, R. Singh, B. Pal, and G. Strbac, "Modeling of pseudo-measurements for distribution system state estimation," in *Proc. IET CIRED Smart Grids for Distribution*, Frankfurt, Germany, 2008, pp. 1–4.

[24] IEEE Standard C37.118-2005, Standard for Synchrophasors for Power Systems. Piscataway, NJ, 2005.

[25] M. W. Davis, R. Broadwater, and J. Hambrick, Modeling and Testing of Unbalanced Loading and Voltage Regulation, National Renewable Energy Laboratory (NREL), Subcontract Report NREL/SR-581-41805, Jul. 2007. [Online]. Available: http://www.nrel.gov/docs/fy07osti/41805.pdf.

[26] D. Montgomery, G. C. Runger, and N. F. Hubele, *Engineering Statistics*, 3rd ed. New York: Wiley, 2004.

[27] M. Powalko, K. Rudion, P. Komarnicki, and J. Blumschein, "Observability of the distribution system," in *Proc. CIRED Int. Conf. Electricity Distribution*, Jun. 2009, pp. 8–11.

[28] M. E. Baran, J. Jung, and T. McDermott, "Topology error identification using branch current state estimation for distribution systems," in *Proc. Transmission and Distribution Conf. Expo., Asia and Pacific*, Oct. 2009, pp. 1–4.

[29] H. Mori, "Optimal allocation of facts devices in distribution systems," in *Proc. IEEE Power Engineering Society Winter Meeting*, Dec. 2001, vol. 2, pp. 936–937.

[30] V. Salehi, S. Afsharnia, and S. Kahrobaee, "Improvement of voltage stability in wind farm connection to distribution network using facts devices," in *Proc. IEEE Conf. Industrial Electronics*, Paris, France, 2006, pp. 4242–4247.

[31] R. Grundbaum, "FACTS for voltage control and power quality improvement in distribution grids," in *Proc. IET Conf. Smart Grids for Distribution*, Aug. 2008, pp. 1–4.

[32] R. Dugan, M. McGranaghan, S. Santoso, and H. Beaty, *Electrical Power Systems Quality*, 2nd ed. New York: McGraw-Hill, 2002.

[33] , IEEE Standard 1547, Standard for Interconnecting Distributed Resources With Electric Power Systems. Piscataway, NJ, 2009.

[34] R. Billinton and S. Jonnavithalu, "A test system for teaching overall power system reliability assessment," *IEEE Trans. Power Syst.*, vol. 11, no. 4, pp. 1670–1676, Nov. 1996.

Daniel A. Haughton (S'09) is from Jamaica and resided in Belize. He received the B.S.E.E degree from the University of South Florida, Tampa, in 2006, and the M.S.E.E. degree from Arizona State University, Tempe, in 2009. He is presently pursuing the Ph.D. degree at Arizona State University.

He has industrial experience with Intel Corp., Chandler, AZ; California ISO, Folsom, CA; Tampa Electric Co., Tampa FL; and Belize Electricity Limited, Belize.

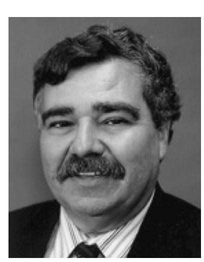

Gerald Thomas Heydt (S'62–M'64–SM'80–F'91–LF'04) is from Las Vegas, NV. He received the Ph.D. degree in electrical engineering from Purdue University, West Lafayette, IN, in 1970.

His industrial experience is with the Commonwealth Edison, Chicago, IL, and E. G. & G., Mercury, NV. He is presently the site director of a power engineering center program at Arizona State University, Tempe, where he is a Regents' Professor.

Dr. Heydt is the 2010 recipient of the Harold Kauffman Award for excellence in distribution engineering. He is a member of the National Academy of Engineering.